PCCP

Absolute electron impact ionization cross-sections for the C_1 to C_4 alcohols

James E. Hudson, Michelle L. Hamilton, Claire Vallance† and Peter W. Harland*

Department of Chemistry, University of Canterbury, Private Bag 4800, Christchurch, New Zealand. E-mail: peter.harland@canterbury.ac.nz

Received 24th April 2003, Accepted 3rd June 2003
First published as an Advance Article on the web 30th June 2003

Absolute total positive-ion electron impact ionization cross-sections from a few eV above threshold to over 200 eV are reported for the C_1 to C_4 alcohols, including the isomers of propanol and butanol. Correlations between measured ionization cross-sections, ionization potential and molecular polarisability volume are explored and compared with data reported previously for perfluorocarbons, nitriles and mixed halocarbons. Small, but reproducible, differences between the isomers of the C_3 and C_4 alcohols have been used to estimate molecular volume polarisabilities for iso- and tertiary butanol. A C–OH functional group contribution to the total ionization cross-section has been deduced in line with bond contributions determined for a range of C–X (where X = C, H, F, Cl, Br, I, CN) bond types previously reported. The reproducibility of the measured cross-sections over the full energy range is better than ±2% and in some cases ±1%. Absolute cross-sections measured with the instrument are in excellent agreement with measurements for the inert gases and N_2 made by several other groups claiming accuracies of around ±5%. Experimental data are compared with calculations using the Deutsch–Märk additivity method, the Binary Encounter Bethe method, and the polarisation model.

1 Introduction

Although electron impact ionization of atoms and molecules has been studied for over eighty years, absolute ionization cross-sections have been measured for a relatively small number of molecules. With the exception of methanol, a recent compilation of absolute total and partial ionization cross-sections does not include any oxygen-containing organic molecules.[1] There have been few studies on the influence of functional group, molecular shape and size, molecular orientation and three-dimensional structure on ionization efficiency.[2–9] Accurate measurements of the total ionization cross-section can be used together with empirical and theoretical relationships to estimate unknown values for other molecular parameters, such as molecular polarisability, and may be used to test theoretical predictions.[10,11] Electron impact ionization plays an important role in many areas of chemistry and physics, including mass spectrometry, plasma processes and gas discharges. Accurate ionization cross-sections are important for understanding the mechanism of the ionization process, and are also required for modelling applications, ranging from studies of fusion plasmas to investigations into radiation effects in medicine and materials science.

The C_1 to C_4 alcohols are widely used both in industry and in the home. Ethanol in particular is a common ingredient in pharmaceuticals and cosmetics, and makes up 10% of the common fuel 'gasohol'. Both n- and iso-propanol are used in cleaning fluids, rubbing alcohol and antifreeze, while butanol is found in plasticizers, resins, industrial solvents and brake fluid. As a result of their widespread use, alcohols are increasingly found in the atmosphere in industrial areas. Methanol and ethanol are also two of the more abundant species in interstellar space, and are thought to be the products of ion-molecule reactions and electron-ion recombination in dense interstellar clouds.

The total ionization cross-section as a function of electron energy has been measured previously for methanol,[12] and for methanol, ethanol and n-propanol,[9,13] although there are no literature measurements for the higher alcohols. In the present work we report cross-sections for the complete set of C_1 to C_4 alcohols, and compare the data with cross-sections calculated using a number of theoretical and empirical models.

2 Models and calculations

There have been many attempts to model electron impact ionization efficiency curves.[11] Two of the more successful theories, the Binary Encounter Bethe model of Kim and Rudd[14–17] and the additivity method of Deutsch and Märk,[18,19] have been used to calculate ionization efficiency curves for comparison with the experimental data and as a test of the theories. In an alternative approach to *ab initio* and semi-empirical models, the maximum ionization cross-section σ_{max} may also be related[10,11] to the molecular volume polarisability α and the ionization potential (or appearance potential) E_0.

$$\sigma_{max} = c'\left(\frac{\alpha}{E_0}\right)^{1/2} \quad \text{and} \quad \sigma_{max} = c''\alpha \qquad (1)$$

where c' and c'' are empirically-determined constants.

One of the fundamental concepts inherent in many theories of electron impact ionization is the 'additivity rule', first elucidated by Otvos and Stevenson[20] in the 1950s. According to the additivity rule, a molecular ionization cross-section can be determined from the sum of the cross-sections of individual atoms, or more generally, of atomic orbitals. The rule is based

† Current address: Physical and Theoretical Chemistry Laboratory, Oxford University, Oxford, UK OX1 3QZ

 DOI: 10.1039/b304456d

on Bethe's observation[21] that the probability of ionization of an electron in an n,l atomic orbital is approximately proportional to the mean-square radius of the orbital. In a variation on the additivity rule, Bobeldijk *et al.*[22] determined a set of bond contributions to the photoionization cross-sections of hydrocarbons and oxygen-containing organic molecules. The contributions were determined from experimental and semi-empirical data, and were found to be in agreement with experiment to within around ±20%. We have recently determined a similar set of bond contributions for electron-impact ionization cross-sections.[6,7] Simple addition of these bond contributions has been shown to predict cross-sections in very close agreement with experiment for a wide range of molecular systems. Bond additivity cross-sections can be rationalised in terms of the same additivity concepts that form the basis of the DM and BEB theories. An empirical relationship, first reported by Lampe, Franklin and Field,[23] between the maximum ionization cross-section and molecular polarisability volume is also consistent with the additive nature of polarisability contributions to the overall molecular polarisability.

3 Experimental

The ionization cell used for these measurements has been described previously[5] and is shown schematically in Fig. 1. The cell is housed in a vacuum chamber with a typical background pressure of $\sim 10^{-7}$ Torr. Permanent rare-earth magnets with nominal pole strength of 6000 Gauss are used to collimate the electrons emitted from a resistively heated rhenium filament which is biased at a potential that determines the electron energy. The effect of the magnetic field on electron path length is small but has been taken into account.[5] The walls of the heated brass collision cell are coated with colloidal graphite in order to prevent surface scattering of charged particles, an important consideration since the cell walls also serve as the ion collector. The trap current is regulated to a preset value, usually 75 nA, using feedback control of the filament current. Since the electron energy distribution exhibits a FWHM of around 1 eV, and the trap current regulation becomes unstable below 20 eV, we have not attempted to report ionization thresholds (appearance energies). However, the cross-section for the ionization of N_2 in the region of the ionization threshold has been measured using a non-regulated filament current supply in order to estimate the effect of contact potentials on the electron energy scale and is shown in Fig. 2. Analar grade

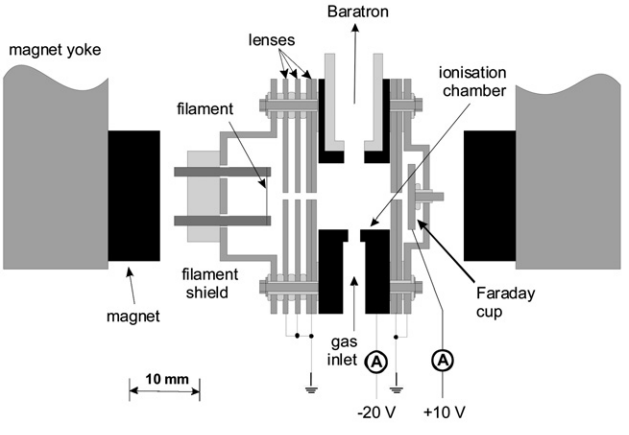

Fig. 1 Scale diagram of the total ionization cell. The plane elements at each end of the ionization chamber are electrically isolated by teflon discs which also form gas-tight seals, all other insulators are of machinable glass ceramic. The ionization chamber body is made of brass which is coated with colloidal graphite on the inside, the Faraday cup is made of gold, and all other elements are made of stainless steel.

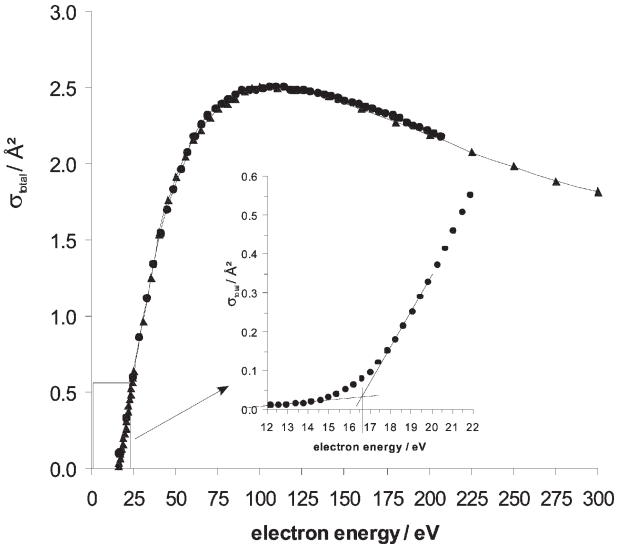

Fig. 2 The total ionization cross-section measured for N_2 (black dots) from 20 to 210 eV compared with the values cited as the "recommended" values in the compilation of cross-section data by Lindsay and Mangan.[1] Absolute cross-section data close to the threshold for N_2 measured using the instrument used in this study are also included in the figure.

alcohols with purities greater than 99.0% were used after vacuum distillation.

Absolute electron ionization cross-sections, σ_i, are calculated from

$$\frac{I^+}{I^-} = n\sigma_i x \qquad (2)$$

where I^+ and I^- are the measured ion and electron currents, n is the number density of the target gas, and x is the path length through the collision cell. Assuming ideal gas behaviour, the above expression can be rewritten:

$$\frac{I^+}{I^-} = \frac{P\sigma_i x}{k_B T} \qquad (3)$$

where P and T are the pressure and temperature of the target gas and k_B is Boltzmann's constant.

In a typical experiment, the pressure of the sample gas is maintained at around 3×10^{-4} Torr, and the electron current is kept below 75 nA in order to preclude space-charge effects. Typical ion currents are in the range 0.1 to 5 nA. The picoammeters used to record the electron and ion currents are computer interfaced through an IEEE parallel bus, while the analogue signals from the thermistor and capacitance manometer (after amplification) are passed to the computer through a commercial 14-bit I/O card. The I/O card is also used to program the electron energy using a Spellman Model MS0.3N, 0 to −300 V, computer-controllable power supply. For each point on an ionization efficiency curve, the electron energy is set and the temperature recorded, following which the ion and electron currents and target gas pressure are measured as the average over ten one-second readings. The resulting ionization efficiency curves are highly reproducible from run to run, even for experiments carried out several weeks apart. The results reported here are the averages of between five and ten repeated determinations for each target gas, made over a period of several months.

Before and after each data run, several measurements were made of the ionization efficiency curve for N_2 which were compared with the data recommended in the compilation by Lindsay and Mangan[1] as an independent assessment of the accuracy of the data (discussed in 4.1 below). This procedure gives us some confidence that the cross sections reported here

for the C_1 to C_4 alcohols are close to the ±4% maximum instrument error determined previously for the apparatus.[5]

4 Results and discussion

4.1 Experimental data

Fig. 2 shows measurements for the absolute ionization cross-section for N_2 from 16 to 207 eV compared to data recommended by Lindsay and Mangan.[1] The inset in Fig. 2 shows measurements of the cross-section from 12 to 22 eV using an unregulated filament supply with the appropriate corrections for the measured electron current as a function of electron energy. The ionization threshold for N_2 (appearance energy for N_2^+) can be estimated by extrapolation to be 16.6 eV which is 1 eV higher than the literature appearance energy of 15.58 eV.[24] The threshold measurement shown in Fig. 2 provides an estimate of the electron energy scale correction for the cell and, in addition, the FWHM electron energy distribution has been estimated to be around 1.2 eV from the curvature around the threshold region. Measurements of the cross-section close to the threshold are subject to more uncertainty due to the small signal levels in this region, and threshold energies are better measured either using a near-monochromatic electron beam or by photoionization. Consequently, only those cross-sections measured from several eV above threshold are reported in this study.

Cross-section tabulations for N_2 and the C_1 to C_4 alcohols are listed in Table 1. Fig. 3 shows a comparison between the measurements reported here for CH_3OH, the averaged Srivastava *et al.*[12] and Duric *et al.*[13] data from the Lindsay and Mangan compilation,[1] the recent measurements reported by

Table 1 Experimental total ionization cross-sections for nitrogen and the alcohols. Maximum values of the cross-section are shown in bold print

	σ/Å^2								
EE/eV	N_2	MeOH	EtOH	1-PrOH	2-PrOH	1-BuOH	2-BuOH	i-BuOH	t-BuOH
16	0.10	0.61	0.75	1.30	1.70	1.70	1.75	1.20	1.52
20	0.34	1.06	1.71	2.74	3.30	3.20	3.40	2.82	3.08
24	0.60	1.63	2.72	4.02	4.97	5.09	5.06	4.71	4.72
28	0.86	2.16	3.65	5.18	6.16	6.55	6.53	6.20	6.27
32	1.12	2.61	4.36	6.14	7.13	7.70	7.75	7.51	7.56
36	1.35	2.98	4.94	6.85	7.79	8.65	8.80	8.70	8.70
41	1.54	3.28	5.44	7.37	8.28	9.47	9.71	9.75	9.71
45	1.70	3.53	5.86	7.84	8.72	10.17	10.48	10.62	10.54
49	1.84	3.76	6.22	8.29	9.10	10.75	11.11	11.05	11.12
53	1.96	3.95	6.51	8.67	9.39	11.20	11.58	11.53	11.55
57	2.08	4.12	6.74	8.97	9.55	11.60	11.90	11.89	11.91
61	2.18	4.26	6.94	9.23	9.66	11.98	12.18	12.20	12.23
65	2.26	4.36	7.14	9.44	9.81	12.23	12.42	12.57	12.55
69	2.32	4.44	7.31	9.60	9.95	12.40	12.60	12.76	12.82
73	2.36	4.49	7.40	9.76	10.07	12.57	12.74	12.97	13.04
77	2.39	4.52	7.45	9.90	10.15	12.70	12.85	13.15	13.20
81	2.43	4.56	7.49	10.00	10.18	12.81	12.95	13.23	13.28
85	2.46	4.59	7.55	10.07	10.20	**12.85**	13.01	13.26	13.32
89	2.48	4.60	**7.60**	10.12	10.22	12.83	13.04	**13.33**	13.34
93	2.49	**4.61**	**7.60**	10.14	**10.24**	12.82	**13.06**	13.29	13.36
97	2.49	**4.61**	7.57	**10.15**	10.23	12.81	13.04	13.26	13.40
101	2.50	**4.61**	7.54	10.14	10.21	12.77	13.03	13.27	**13.41**
105	2.50	4.60	7.51	10.12	10.17	12.76	13.03	13.27	13.37
109	**2.50**	4.59	7.49	10.07	10.12	12.71	12.95	13.17	13.33
113	2.50	4.56	7.47	10.03	10.06	12.60	12.85	13.07	13.31
117	2.49	4.53	7.41	10.01	10.00	12.54	12.82	13.06	13.30
122	2.48	4.50	7.35	9.99	9.95	12.54	12.81	13.02	13.26
126	2.48	4.48	7.30	9.95	9.90	12.50	12.76	13.00	13.18
130	2.48	4.46	7.28	9.91	9.83	12.40	12.65	12.95	13.10
134	2.46	4.44	7.25	9.85	9.75	12.27	12.56	12.83	13.06
138	2.46	4.41	7.21	9.79	9.69	12.21	12.49	12.75	13.00
142	2.44	4.38	7.16	9.72	9.65	12.19	12.41	12.61	12.89
146	2.43	4.36	7.12	9.66	9.62	12.13	12.29	12.49	12.75
150	2.42	4.33	7.09	9.60	9.56	12.01	12.13	12.46	12.63
154	2.41	4.31	7.06	9.54	9.50	11.89	11.99	12.38	12.54
158	2.39	4.29	7.01	9.49	9.45	11.76	11.90	12.21	12.51
162	2.38	4.25	6.96	9.43	9.37	11.68	11.86	12.19	12.48
166	2.36	4.23	6.92	9.36	9.29	11.63	11.81	12.16	12.42
170	2.35	4.19	6.87	9.27	9.22	11.56	11.73	12.05	12.33
174	2.34	4.15	6.81	9.20	9.15	11.44	11.62	12.04	12.23
178	2.32	4.11	6.76	9.12	9.08	11.28	11.47	11.93	12.13
182	2.30	4.08	6.71	9.05	9.01	11.14	11.34	11.87	12.04
186	2.28	4.04	6.65	9.01	8.96	11.02	11.25	11.80	11.96
190	2.25	4.00	6.59	8.97	8.89	10.93	11.21	11.69	11.89
194	2.24	3.98	6.53	8.92	8.83	10.81	11.20	11.56	11.81
198	2.22	3.95	6.49	8.87	8.75	10.72	11.20	11.48	11.71
203	2.20	3.92	6.43	8.82	8.68	10.65	11.15	11.41	11.61
207	2.18	3.89	6.35	8.76	8.59	10.55	11.08	11.28	11.47

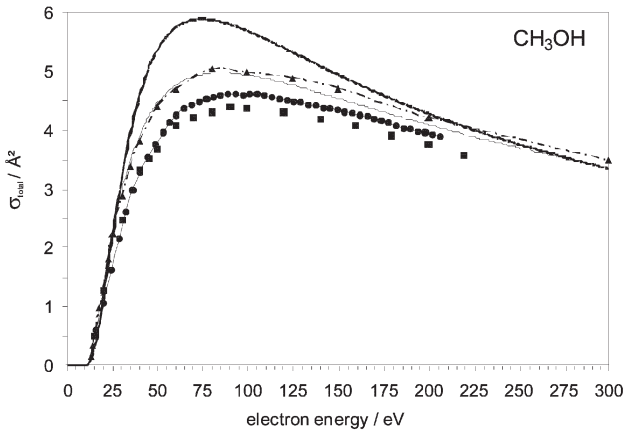

Fig. 3 Experimental and calculated total ionization cross-sections for CH_3OH: this work (●); data recommended in Lindsay and Mangan[1] (■); Rejoub *et al.*[9] (▲); BEB calculation (thin line); DM calculation (thick line).

Rejoub *et al.*,[9] and calculations carried out using the BEB and DM methods. The measurements reported here agree well with the averaged data set from near threshold to 45 eV after which our values are consistently 0.2 Å^2 higher (4 to 5%). The original cross-section data reported by Strivastava *et al.* are relative values using He as the reference with an estimated uncertainty on the CH_3OH cross-sections of ±15%. Above 90 eV their reported cross-sections are in excellent accord with the measurements reported here although there is a marked deviation below 90 eV which is reflected in the curve shown in Fig. 3. Duric *et al.* employed a parallel plate collector method and claim an uncertainty of ±10% in their cross-sections. Their data below 50 eV are in excellent accord with ours but above 50 eV their cross-sections are consistently 0.2 to 0.3 Å^2 lower as reflected in the average recommended by Lindsay and Mangan. Although Duric *et al.* did not report cross-section data for other alcohols, they stated that careful measurements showed that the maximum total ionization cross-sections for ethanol and n-propanol were 1.55 and 1.78 times higher than for methanol, respectively. This would translate into values of 7.15 Å^2 for ethanol and 8.21 Å^2 for n-propanol compared to the values of 7.60 and 10.15 Å^2 reported here. The summed partial cross-section data recently reported by Rejoub *et al.*[9] are also shown in the figure. Their maximum cross-section, 4.975 Å^2, is 8% higher than the value measured here and 13% higher than the data set recommended by Lindsay and Mangan.[1] Since Rejoub *et al.*[9] claim an accuracy of ±6–8% the data reported here are in agreement with theirs within the combined uncertainties.

Fig. 4 illustrates the high degree of reproducibility for this experiment; the mean of ten measurements for CH_3OH collected over the space of a week (heavy line) is plotted with the plus and minus one-standard-deviation curves (thin lines). The difference plot included in the figure shows that the standard deviation is less than 1.5% over the electron energy range for which measurements were made. Measured ionization efficiency curves for ethanol and the C_3 alcohols are shown in Fig. 5,

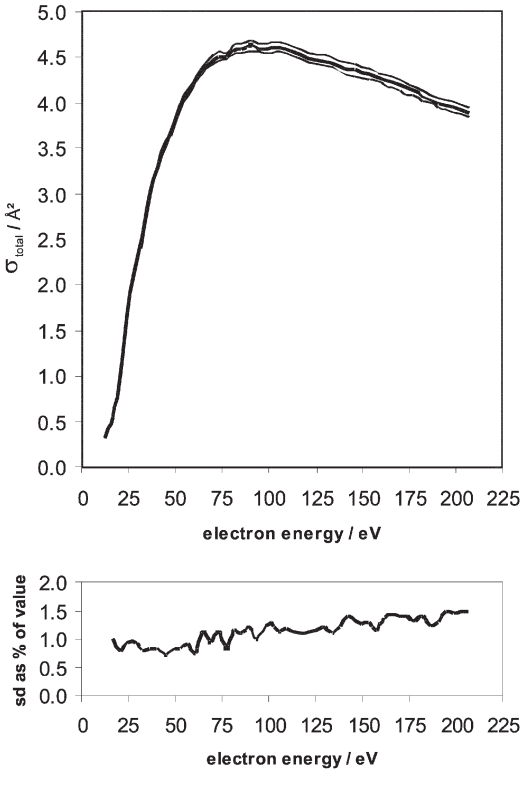

Fig. 4 Total ionization cross-section for CH_3OH averaged over ten runs (thick line) with one standard deviation (thin lines). The standard deviation as a percentage of the cross-section is shown in the lower plot.

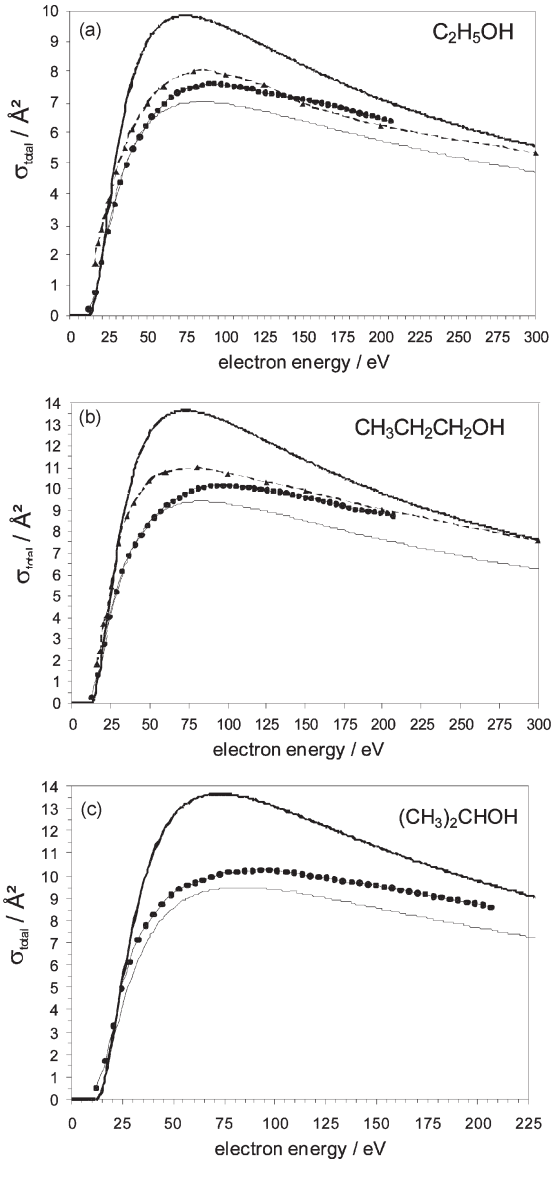

Fig. 5 Experimental and calculated total ionization cross-sections for ethanol and the isomers of propanol: this work (●); Rejoub *et al.*[9] (▲); BEB calculation (thin line); DM calculation (thick line).

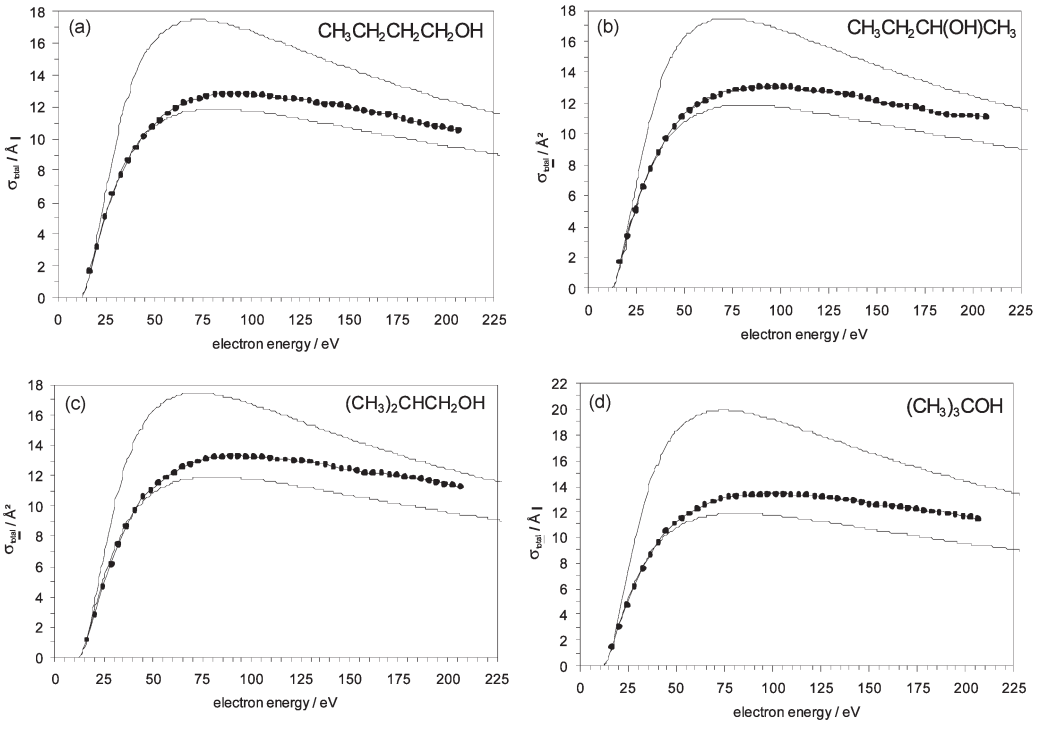

Fig. 6 Experimental and calculated total ionization cross-sections for the isomers of butanol: this work (●); BEB calculation (thin line); DM calculation (thick line).

together with the results of the BEB and DM calculations and the experimental results of Rejoub *et al.*[9] for ethanol and n-propanol. The corresponding plots for the four C_4 isomers are shown in Fig. 6.

There is good agreement between the ethanol data reported here and the data reported by Rejoub *et al.*[9] at the higher electron energies, although there appears to be a significant deviation for the lower electron energies. The summed partial cross-section data using Table 2 from Rejoub *et al.*[9] gives a maximum total cross-section of 8.00 Å^2 at 80 eV compared to a maximum of 7.60 Å^2 at 90 eV reported here. The difference is well within the combined errors for these experiments although the differences in the shapes of the curves at the lower electron energies cannot be readily explained. The methanol curve of Rejoub *et al.* exhibits a smaller deviation from our data and from that recommended by Lindsay and Mangan[1] at the lower electron energies although it is far greater for n-propanol, also shown in Fig. 5.

The maximum cross-section measured for the alcohols and the values calculated using the BEB, DM and polarisation models are listed in Table 2 with the percentage deviations of the calculated values from experiment shown in parentheses. Since the polarisation model requires knowledge of the molecular volume polarisability, maximum cross-sections could not be calculated for iso- or tertiary butanol, for which this information is not available. With the exception of methanol, for which the BEB model over-estimates the maximum cross-section by 8%, the BEB model consistently under-estimates the cross-sections above 45 eV by 7–12%. The DM model over-estimates the cross-section for all alcohols over the full range of electron energies by 27–48% and, in addition, the shape of the ionization efficiency curve is not well reproduced, with the maximum value of the cross-section occurring at electron energies 25–40 eV lower than the experimental values. These conclusions can be compared with our previous work on fluorocarbons, nitriles, and chlorocarbons. We found that the BEB model performed well for the CF_4 to C_4F_8 perfluorocarbons but generally under-estimated cross-sections for small mixed-halogen molecules with heavier atoms, such as chlorine or bromine. The BEB model consistently under-estimates cross-sections for the chlorocarbons by 30–40% while the DM model gives better agreement on the cross-sections but under-estimates the electron energy corresponding to the maxima. A recent paper by Lindsay *et al.*[25] on partial and total ionization cross-sections for N_2O, H_2S and CS_2 reported good accord between the BEB calculations and the experimental values for N_2O but a considerable under-estimation of the cross-sections for H_2S and CS_2.[25]

Table 2 Experimental and calculated (BEB and DM) maximum total ionization cross-sections for the alcohols expressed in units of Å^2 (1 Å^2 = 1×10^{-20} m^2). The percentage differences between calculated and experimental values are shown in parentheses

Molecule	σ_{max}(expt)	σ_{max}(BEB)	σ_{max}(DM)	σ_{max}(pol)
CH_3OH	4.61	4.98 (+8.0)	5.88 (+27.5)	4.96 (+7.6)
C_2H_5OH	7.60	7.00 (−7.9)	9.82 (+29.2)	7.75 (+2.0)
1-C_3H_7OH	10.15	9.41 (−7.3)	13.65 (+34.5)	9.86 (−2.9)
2-C_3H_7OH	10.24	9.48 (−7.4)	13.66 (+33.4)	10.63 (+3.8)
1-C_4H_9OH	12.85	11.90 (−7.4)	17.47 (+36.0)	12.90 (+0.4)
2-C_4H_9OH	13.06	11.88 (−9.0)	17.48 (+33.8)	12.91 (−1.1)
iso-C_4H_9OH	13.33	11.94 (−10.4)	17.48 (+31.1)	
tert-C_4H_9OH	13.41	11.87 (−11.5)	19.90 (+48.4)	

The simple polarisability model for maximum cross-sections works well for all molecules for which polarisability data are available.[8] The model is not an alternative to the BEB and DM models as it does not adequately predict the shape of the cross-section *versus* electron energy dependence. However, the empirical calculations do provide an independent estimate of the maximum cross-section for comparison with experiment and theory and yield a result that is generally in good accord with experiment.

4.2 Discussion

We have previously reported correlations between the maximum ionization cross-section and molecular electrostatic

parameters such as molecular volume polarisability, α, and $(\alpha/E_0)^{1/2}$, where E_0 is the molecular ionization threshold or appearance energy. Fig. 7a shows a plot of the experimental, DM and BEB maximum total ionization cross-sections for the alcohols *versus* molecular volume polarisability (where available). A least-squares fit through the experimental points (circles) extrapolates close to the origin, while the BEB (squares) and DM data exhibit significant negative and positive intercepts, respectively. The fit provides a relationship relating the maximum total ionization cross-section (in Å^2) to the molecular polarisability (in Å^3) for the alcohols studied.

$$\sigma_{max} = 1.479\ \alpha - 0.0934 \quad (R^2 = 0.997) \qquad (4)$$

A similar fit forced through the origin yields

$$\sigma_{max} = 1.466\ \alpha \quad (R^2 = 0.997) \qquad (5)$$

This compares favourably with previously reported data from other groups, and also with our own earlier measurements, for which a similar procedure yielded the relationship $\sigma_{max} = 1.455\ \alpha$ with $R^2 = 0.989$. Using eqn. (5), the polarisabilities for iso- and tert-butanol are estimated to be 9.093 and 9.147 Å^3, respectively.

The experimental maximum total ionization cross-sections are plotted against the square root of the ratio of polarisability to appearance energy in Fig. 7b; the least squares fit shows a high degree of correlation with

$$\sigma_{max} = 22.25\ (\alpha/E_0)^{1/2} - 7.83 \quad (R^2 = 0.994) \qquad (6)$$

Fig. 8 shows a plot of the measured maximum total ionization cross-section for the alcohols *versus* the number of carbon

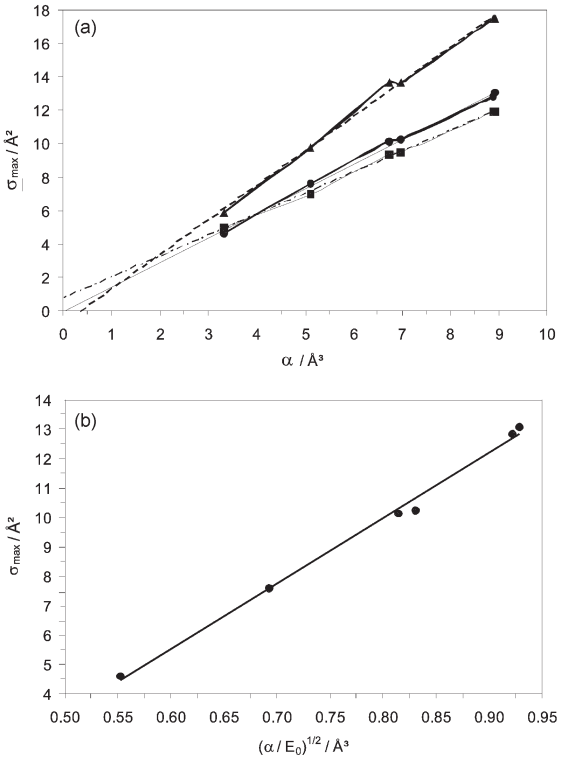

Fig. 7 (a) Plot of the maximum total ionization cross-section for the alcohols *versus* molecular volume polarisabilty: (●) this work; (▲) DM calculations; (■) BEB calculations. The dashed lines are extrapolated least squares fits through the DM and BEB data points and the thin line is through the experimental data points. (b) Plot of the maximum total ionization cross-section for the alcohols *versus* the square root of the ratio of molecular volume polarisability to the ionization threshold for the molecular ion. The thick line is a least squares fit to the data points.

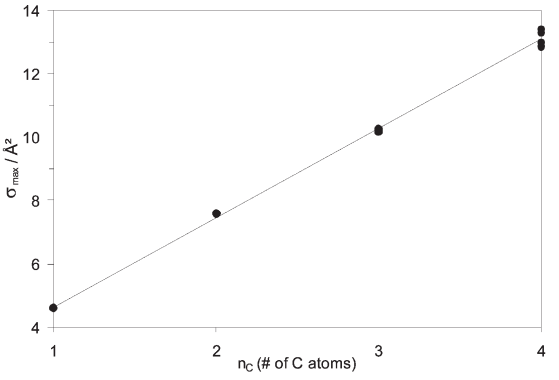

Fig. 8 Plot of the maximum total ionization cross-sections for the alcohols *versus* the number of carbon atoms in the aliphatic backbone.

atoms. The best fit line through the data points is given by

$$\sigma_{max} = 2.83\ n_C + 1.81 \quad (R^2 = 0.997).$$

The constant increment between the data points, given by the slope as 2.83, corresponds to the contribution of a C–CH$_2$ grouping to the maximum cross-section, *i.e.*, a C–C single bond plus two C–H bonds. In previous studies on the effect of carbon chain length and functional group substitution on ionization cross-section a number of bond contributions have been determined (see Table 3) and shown to be useful in predicting cross-sections.[6,7] No allowance was made in the earlier work for isomeric variations, since the focus at that time was on the effects of halogen and nitrile substituents on the cross-section. The mean contributions to the maximum total cross-section of the C–C bond and the C–H were determined independently to be 1.0 Å. Combining these gives a C–CH$_2$ group contribution of 3.0 Å^2. Although this averaged value is 6% higher than the C–CH$_2$ group contribution deduced directly from this series of alcohols, it is still well within the uncertainty stated for most experimental studies. The intercept from Fig. 8, which represents the C–OH group contribution to the maximum total ionization cross-section of 1.8 Å^2, has been included in Table 3 with the C–CH$_2$ group contribution.

The mean values for the maximum total ionization cross-sections determined for the isomers of the C_3 and C_4 alcohols listed in Tables 1 and 2 appear to show a trend. The normal alcohols exhibit the lowest value and the more branched alcohols have higher values for the maximum cross-section. While the difference of 0.09 Å^2 (0.1 Å^2) between the isomers of propanol is not statistically significant, the models do predict a difference of this magnitude and direction. The same

Table 3 Additive bond contributions to the maximum ionization cross-section for reported in ref. 3 and the value for C–OH deduced from Fig. 8

Bond	Cross-section component/Å^2
C–H	1.0
C–F	1.1
C–Cl	3.8 for C = 1 4.4 for C > 1
C–Br	4.5
C–I	7.3
C–CN	3.0
C–C	1.0
C=C	1.5
C≡C	1.7
C–CH$_2$	2.8
C–OH	1.8

considerations apply to the C_4 alcohols where there is a 4% increase in measured cross-section from 1-butanol to t-butanol. The BEB model does not indicate an isomeric trend whereas the DM model predicts a significant difference between t-butanol and the other isomers. Since there are differences in the reported polarisabilities between isomers, increasing polarisability with branching, the polarisability model would predict a similar trend in cross-section. This may become more pronounced for larger molecules with a wider range of three-dimensional shapes and further work is in progress.

Conclusion

Total absolute ionization cross-sections from 16 to 200 eV have been measured for the C_1 to C_4 alcohols including all isomers and compared to the predictions of the BEB, DM and polarisation models and to previously reported data. Measurements for iso-propanol and the C_4 alcohols are reported for the first time. The measurements reported here, combined with previous studies, have been used to prepare a table of component bond and group contributions to the total ionization cross-section that may be used to estimate maximum total ionization cross-sections with a high degree of confidence. Application of relationships between the maximum total ionization cross-section and polarisability derived through the polarisation model are in good agreement with comparisons made with the halocarbons in previous studies. Estimates for previously unreported molecular volume polarisabilities for two of the C_4 isomers using these relationships are included in the text. In addition, small but reproducible differences between the maximum total ionization cross-section for the C_3 and C_4 isomers suggest that such differences for larger molecules with a greater diversity of geometric isomerism may be more significant and be shown to correlate with molecular shape and differences in polarisability.

Acknowledgements

PWH should like to acknowledge the Marsden Fund for support of this work through grant 99-UOC-032 PSE. CV acknowledges the support of the Royal Society through the award of a University Research Fellowship.

References

1 B. G. Lindsay and M. A. Mangan, *Landolt–Börnstein, Photon- and electron-interactions with molecules: Ionization and dissociation*, ed. Y. Itikawa, Springer-Verlag, Berlin–Heidelberg, 2003, vol. I/17C, ch. 5.
2 C. G. Aitken, D. A. Blunt and P. W. Harland, *J. Chem. Phys.*, 1994, **101**, 11 074.
3 C. G. Aitken, D. A. Blunt and P. W. Harland, *Int. J. Mass Spectrom. Ion Processes*, 1995, **149/150**, 279.
4 C. Vallance, R. G. A. R. Maclagan and P. W. Harland, *J. Phys. Chem. A*, 1997, **101**, 3505.
5 C. Vallance, S. A. Harris, J. E. Hudson and P. W. Harland, *J. Phys. B*, 1997, **30**, 2465.
6 M. Bart, P. W. Harland, J. E. Hudson and C. Vallance, *Phys. Chem. Chem. Phys.*, 2001, **3**, 800.
7 J. E. Hudson, C. Vallance, M. Bart and P. W. Harland, *J. Phys. B*, 2001, **34**, 3025.
8 R. Rejoub, B. G. Lindsay and R. F. Stebbings, *J. Chem. Phys.*, 2002, **117**, 6450.
9 R. Rejoub, C. D. Morton, B. G. Lindsay and R. F. Stebbings, *J. Chem. Phys.*, 2003, **118**, 1756.
10 P. W. Harland and C. Vallance, *Int. J. Mass Spectrom. Ion Processes*, 1997, **171**, 173.
11 P. W. Harland and C. Vallance, in *Advances in Gas-Phase Ion Chemistry*, eds. N. G. Adams and L. M. Babcock, JAI Press Ltd., London, 1998, vol. 3.
12 S. K. Srivastava, E. Krishnakumar, A. F. Fucaloro and T. van Note, *J. Geophys. Res.*, 1996, **101**, 26 155.
13 N. Duric, I. Cadez and M. Kurepa, *Fizika 21*, 1989, **4**, 339.
14 Y. K. Kim and M. E. Rudd, *Phys. Rev. A.*, 1994, **50**, 3954.
15 W. Hwang, Y. K. Lim and M. E. Rudd, *J. Chem. Phys.*, 1996, **104**, 2956.
16 Y. K. Kim, W. Hwang, N. M. Weinberger, M. A. Ali and M. E. Rudd, *J. Chem. Phys.*, 1997, **106**, 1026.
17 See BEB database at http://physics.nist.gov/cgi-bin/Ionization/.
18 D. Margreiter, H. Deutsch and T. D. Märk, *Int. J. Mass Spectrom. Ion Processes*, 1994, **139**, 127.
19 H. Deutsch, K. Becker, S. Matt and T. D. Märk, *Int. J. Mass Spectrom. Ion Processes*, 2000, **197**, 37.
20 J. W. Otvos and D. P. Stevenson, *J. Am. Chem. Soc.*, 1956, **78**, 546.
21 H. Bethe, *Ann. Physik*, 1930, **5**, 325.
22 M. Bobeldijk, W. J. Van der Zande and P. G. Kistermaker, *Chem. Phys.*, 1994, **179**, 125.
23 F. W. Lampe, J. L. Franklin and F. H. Field, *J. Am. Chem. Soc.*, 1957, **79**, 6129.
24 *NIST Chemistry Webbook*, http://webbook.nist.gov/chemistry/, 2003.
25 B. G. Lindsay, R. Rejoub and R. F. Stebbings, *J. Chem. Phys.*, 2003, **118**, 5894.